

Computed Tomography Imaging for Novel Therapies of Chronic Obstructive Pulmonary Disease

Hans-Ulrich Kauczor, MD, PhD,*†‡ Mark O. Wielpütz, MD,*†‡
Bertram J. Jobst, MD,*†‡ Oliver Weinheimer, PhD,*†‡
Daniela Gompelmann, MD,†§ Felix J.F. Herth, MD, PhD,†§
and Claus P. Heussel, MD, PhD*†‡

Abstract: Novel therapeutic options in chronic obstructive pulmonary disease (COPD) require delicate patient selection and thus demand for expert radiologists visually and quantitatively evaluating high-resolution computed tomography (CT) with additional functional acquisitions such as paired inspiratory-expiratory scans or dynamic airway CT. The differentiation between emphysema-dominant and airway-dominant COPD phenotypes by imaging has immediate clinical value for patient management. Assessment of emphysema severity, distribution patterns, and fissure integrity are essential for stratifying patients for different surgical and endoscopic lung volume reduction procedures. This is supported by quantitative software-based postprocessing of CT data sets, which delivers objective emphysema and airway remodelling metrics. However, the significant impact of scanning and reconstruction parameters, as well as intersoftware variability still hamper comparability between sites and studies. In earlier stage COPD imaging, it is less clear as to what extent quantitative CT might impact decision making and therapy follow-up, as emphysema progression is too slow to realistically be useful as a mid-term outcome measure in an individual, and longitudinal data on airway remodelling are still very limited.

Key Words: chronic obstructive pulmonary disease, computed tomography, functional imaging, quantitative imaging, lung volume reduction

(*J Thorac Imaging* 2019;34:202–213)

Chronic obstructive pulmonary disease (COPD) is a multifactorial disorder that is most often caused by inhalational toxins and whose main manifestations adversely affect the lungs.¹ In the near future, COPD is predicted to be the leading cause of pulmonary mortality worldwide.¹ Pulmonary morbidity in COPD is in close

interdependency with other diseases of overlapping causality, such as lung cancer, occupational lung disease, atherosclerosis, coronary heart disease, and stroke.^{1,2} A precise assessment of COPD disease severity is not only pivotal for therapy decision making with regard to COPD, but also has implications for treatment of confounding diseases such as lung cancer. Recent studies have proposed that the interactions between multiple possible toxins, environmental factors, and behavioral and genetic differences cause the structural and functional changes of the lungs that ultimately lead to obstructive symptoms. These cannot be predicted or sufficiently graded by pulmonary function testing alone.³ Thus, cross-sectional imaging is increasingly being used to assess structural and functional lung changes in COPD, which is mainly characterized by 2 components, airway remodeling and emphysema.⁴ However, these aspects may coexist and contribute to symptoms to a different degree in individual patients, and this somewhat arbitrary separation is mainly due to the limited resolution of clinical computed tomography (CT), which cannot display most of the subsegmental airway generations.^{4,5} Further, emphysema visible on CT correlates histopathologically with large parts of the lung tissue that have already been destroyed. Because airway remodeling is thought to be at least in part reversible, whereas to date emphysema marks an irreversible destruction, the separation into an airway-dominant and an emphysema-dominant disease has increased the value for directing therapy in COPD. Novel therapy regimes, especially endoscopic lung volume reduction (ELVR) techniques, require specific work-up with high-resolution CT in order to effectively treat patients with emphysema. This article aims to give an overview of CT applications for directing therapy in COPD and offers a future perspective on imaging biomarkers for therapy assessment in COPD.

PHENOTYPING

COPD is defined on the basis of spirometric evidence of airway obstruction; the Global Obstructive Lung Disease (GOLD) system is used to identify and classify the severity of postbronchodilator airflow limitation in COPD.¹ GOLD stage I includes patients with a ratio of forced expiratory volume in 1 second (FEV1) to forced vital capacity (FVC) of <0.7 but with preserved FEV1, and GOLD stages II, III, and IV when the FEV1/FVC ratio is <0.7 and FEV1 is <80%, 50%, and 30% of the predicted values, respectively. Obviously, lung function measurements are global and do not provide any information about either the localization or the cause of the obstruction. Thus, COPD encompasses emphysema, chronic bronchitis, reversible or irreversible small airways

From the *Department of Diagnostic and Interventional Radiology, University Hospital of Heidelberg; †Translational Lung Research Center (TLRC), German Center for Lung Research (DZL), University of Heidelberg; ‡Department of Diagnostic and Interventional Radiology with Nuclear Medicine; and §Department of Respiratory and Critical Care Medicine, Thoraxklinik at University of Heidelberg, Heidelberg, Germany.

Supported in part by grants from the German Federal Ministry of Education and Research (82DZL001A6, 82DZL002A1, 82DZL004A1, 82DZL005A1). Parts of the airway segmentation algorithm from YACTA presented in this review have been licensed to the company IMBIO, LLC.

The authors declare no conflicts of interest.

Correspondence to: Hans-Ulrich Kauczor, MD, PhD, Department of Diagnostic and Interventional Radiology, University Hospital of Heidelberg, Im Neuenheimer Feld 110, Heidelberg 69120, Germany (e-mail: hu.kauczor@med.uni-heidelberg.de).

Copyright © 2018 Wolters Kluwer Health, Inc. All rights reserved.
DOI: 10.1097/RTI.0000000000000378

obstruction, as well as dynamic large airway instability, and patients with identical GOLD stages may show substantially different morphology at CT. This observation has led to the introduction of CT phenotypes for subjects with and even at risk for airway obstruction, and the terms of emphysema-dominant and airway-dominant phenotype were coined. In 2015, the Fleischner Society published a statement on the definition of these (sub-)phenotypes at CT.⁴ However, whether these CT-phenotypes actually also reflect important differences in the underlying pathophysiology and genomic profile is still under investigation.

The emphysema-dominant phenotype mainly consists of centrilobular emphysema characterized by small well-defined or poorly defined areas of low attenuation surrounded by normal lung with differences in extent (trace occupying <0.5% of a lung zone; mild occupying of 0.5% to 5% of a lung zone; moderate with > 5% of any lung zone). This pattern of emphysema shows a good correlation with histology and micro CT.^{6,7} With progression, the areas of emphysema will coalesce, and signs of hyperinflation will appear. Thus, confluent centrilobular emphysema refers to coalescent lobular lucencies without hyperexpansion or distortion of pulmonary architecture, whereas advanced destructive emphysema is based on panlobular lucencies with hyperexpansion and architectural distortion. At the same time, the term panlobular emphysema should only be used for patients with alpha-1-antitrypsin deficiency. Paraseptal emphysema with well-demarcated juxtaleural lucencies aligned in a row along the pleural margins is listed as a separate entity and subcategorized as mild or substantial (Fig. 1). The novel therapies will primarily target patients with confluent centrilobular and advanced destructive emphysema, especially when the distribution of these changes is heterogenous. Heterogeneity is best assessed by differences in the emphysema index between the target and the ipsilateral lobe of > 10% or 15%.

The airway-dominant phenotype refers to obvious abnormalities of the airways in the absence of emphysema as well as the clear predominance of abnormalities of the airways in the presence of emphysema. Abnormalities are noted separately for bronchial as well as small airway disease. Bronchi will exhibit wall thickening, sometimes associated with a reduction, sometimes with dilation of the lumen. Normal small airways—by definition—are not visible at CT. When diseased, centrilobular micronodules and tree-in-bud patterns are direct signs of small airway disease. Air-trapping, especially with the use of expiratory CT, is an indirect sign.^{8,9} According to the statement of the Fleischner Society, abnormalities of the large airways, such as tracheobronchomegaly, saber sheath trachea, and tracheobronchial outpouchings, are just regarded as associated features as well as bronchiectasis, which should be clearly separated from the airway-dominant phenotype. In general, patients with an airway-dominant phenotype will not be obvious candidates for the novel endobronchial therapies that aim at hyperinflation reduction. However, patients with small airways' disease identified by air trapping should deserve special attention, as this might be considered as a precursor of centrilobular emphysema, and the potential benefit of early treatment by novel treatment options should be investigated.

QUANTITATIVE IMAGING BIOMARKERS

Different quantitative CT (QCT) techniques have been used to measure structural changes in the lung parenchyma

and in the tracheobronchial-tree. To obtain accurate and precise QCT results, it is essential to follow a standardized CT scanning protocol.^{3,10} Presence and extent of emphysema can be quantified on inspiratory CT scans by the percent of lung voxels with an attenuation <−950 HU (emphysema index, Insp_{-950}).^{6,11} Subdivisions of the lung are the division into lung lobes or into cortical and medullary lung regions (Fig. 2, subject S4). The determination of these lung subdivisions and all QCT techniques described in this section can be carried out fully automated by dedicated software tools^{12–14}—if necessary manual corrections of the segmentation results are feasible in such tools. This color-coded markup of emphysema distribution simplifies the planning of an eventual surgical approach.¹⁵ Lobe-based emphysema analysis allows a quantitative description of the local distribution of low-attenuation areas, for example, the subject S1 in Figure 1 has mainly apical and subject S7 in Figure 3 predominantly basal localized emphysematous lung destruction. This is quantified by high Insp_{-950} values for the upper lobes and for the lower lobes. Beside lobe segmentation, the determination of fissure integrity (FI) is an important area of research, as FI plays a key role in selecting patients for interventional emphysema therapy.^{13,16,17} A completely different emphysema distribution is shown by the CT images of the 2 subjects in Figure 1 (S2 and S3); here, we see a more cortical predominant emphysema type on the one hand and a medullary predominant emphysema type on the other hand—well described on the increased emphysema index Insp_{-950} for the cortical and medullary regions, respectively.¹⁵

Quantification of the local distribution of gas trapping is achievable by the determination of the percentage of lung voxels <−856 HU (Exp_{-856}) on expiratory CT scans. If paired inspiratory and expiratory scans are acquired, the ratio of expiratory to inspiratory mean lung attenuation (E/I MLA) can be used as a further gas-trapping measure. These 2 approaches are markers of small airway disease in smokers with and without COPD but are not able to separate gas trapping due to emphysema from gas trapping due to small airway disease.^{11,18} Another technique tries to exclude emphysematous areas and determines the difference between the relative lung volume change in the attenuation range of −950 to −856 HU on expiratory and inspiratory scans ($\text{RVC}_{856-950}$); the lower threshold was adopted to eliminate the influence of emphysema; it has been shown that this index correlated closely with airway dysfunction in COPD regardless of the degree of emphysema.^{11,18}

A computationally more complex approach is the parametric response map (PRM) method developed by Galbán and colleagues, a voxel-wise image analysis technique that does not only require segmentation but also registration for assessing the COPD phenotypes.¹⁹ The PRM method spatially aligns the expiratory to the inspiratory scan by a deformable volumetric registration process. Thereafter, the classification of lung voxels can be carried out by using the expiratory and inspiratory attenuation value for every voxel. This allows classifying lung voxels as normal parenchyma ($\text{PRM}^{\text{Normal}}$), functional small-airway disease (PRM^{ISAD}), and emphysema (PRM^{Emph}) (Fig. 4). Galbán's PRM method has been integrated with advanced registration techniques in commercial software systems like the Lung Density Analysis (LDA) software (Imbio, LLC, Minneapolis, MN), the Pulmonary Workstation 2.0 (VIDA Diagnostics, Coralville, IA), the LungQ software (Thirona, Nijmegen, Netherlands), or the research software system YACTA (University of Heidelberg, Heidelberg, Germany).

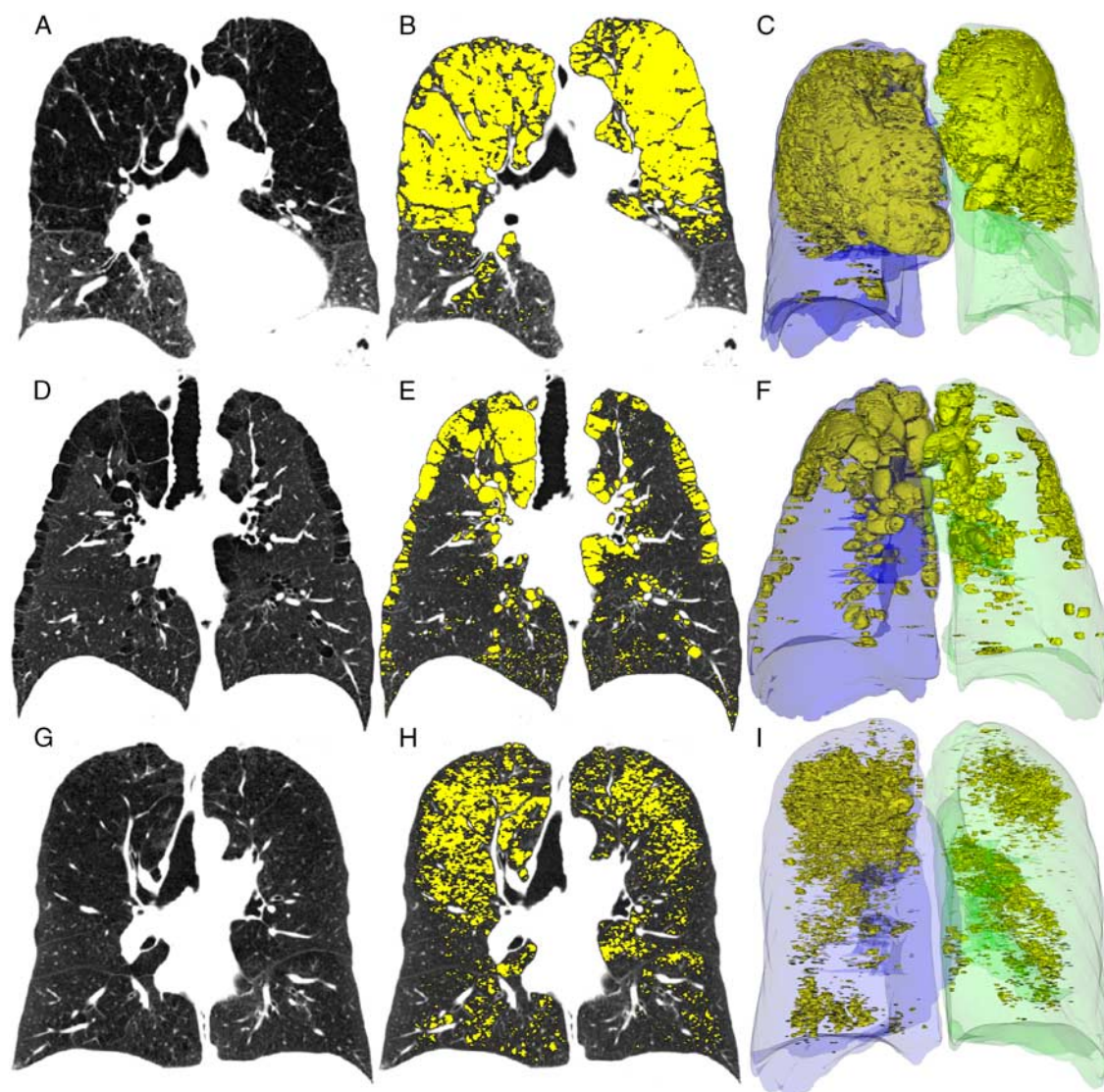


FIGURE 1. A–C, CT of a 71-year-old female COPD patient (subject S1), GOLD status 3. Most of the emphysema (yellow) is localized in the apical regions. Insp_{-950} for the whole lung is 41%, Insp_{-950} for RUL, RML, RLL and LUL, LLL is 66%, 35%, 7% and 60%, 2%, respectively. D–F, CT of a 50-year-old male COPD patient (S2), GOLD status 1. Emphysema (yellow) is predominantly localized in the cortical regions of the lung. Insp_{-950} for the whole lung is 12%; 73% of the emphysema is in the cortical regions. G–I, CT of a 57-year-old female COPD patient (S3), GOLD status 3. Emphysema is mainly localized in the medullary lung regions. Insp_{-950} for the whole lung is 14%; 80% of the emphysema is in the medullary regions. COPD indicates chronic obstructive pulmonary disease; LLL, left lower lobe; LUL, left upper lobe; RLL, right lower lobe; RML, right middle lobe; RUL, right upper lobe.

It has been shown in multiple studies that PRM serves as a valuable measure of disease. The COPDGene and SPIROMICS studies have both integrated PRM as part of their trials.^{20,21} Further processing is available for quantification of air trapping from paired inspiratory and expiratory scans with adjustment of CT image quality problems.²²

Another way to quantify the contribution of airway disease in COPD is the direct analysis of the airway tree on inspiratory CT scans. For this, the lumen of the tracheobronchial tree will be segmented, the skeleton of the segmentation determined, and a graph representation of the airway tree generated. Thereafter, the airways can be labeled according to the lobes they belong to. The direction vector of an airway is calculable by the underlying graph representation and the skeleton. Thus, it is possible to calculate orthogonal planes for

every airway, more precisely for every skeleton point.^{5,23–25} Lumen, wall thickness, and wall percentage values can be determined for the whole tree at every skeleton position, that is, generation specific. An elegant way to condense the amount of the generated data into an aggregated metric is to calculate the wall area for a theoretical airway with an internal perimeter of 10 mm (AWT-Pi10) by regression analysis.²⁶ Average values for the whole tree and for the individual lobes can be determined for AWT-Pi10 and wall percentage values. Taper index calculation allows the quantification of bronchiectasis²⁵ (Fig. 5). All presented imaging biomarkers are potentially useful for therapy monitoring, and there is yet no consensus on which are most useful. Importantly, both low-attenuation areas and airway wall remodeling on QCT contribute additively to clinical disease severity measured by the BODE index in

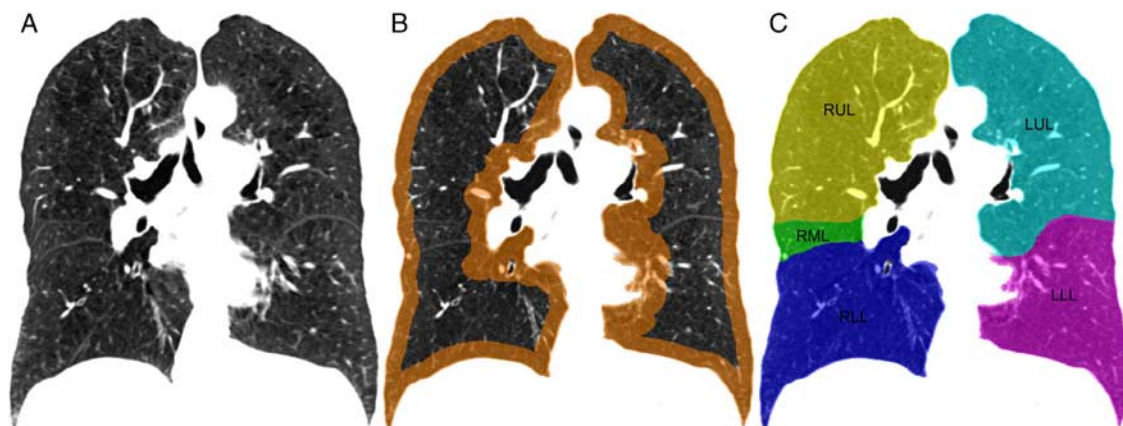


FIGURE 2. A–C, CT of a 68-year-old female COPD patient (S4), GOLD status 3, and lung volume = 5884 cm³; Insp₋₉₅₀ for the whole lung is 21%. B, Cortical regions containing 50% of the overall segmented lung voxels marked. C, Labeled lung lobes, right upper lobe (RUL, volume = 1470 cm³, Insp₋₉₅₀ = 26%), right middle lobe (RML, volume = 437 cm³, Insp₋₉₅₀ = 28%), right lower lobe (RLL, volume = 1342 cm³, Insp₋₉₅₀ = 25%), left upper lobe (LUL, volume = 1253 cm³, Insp₋₉₅₀ = 14%), and left lower lobe (LLL, volume = 1383 cm³, Insp₋₉₅₀ = 14%).

COPD,²⁷ and both also independently increase the risk for COPD exacerbation.²⁸ The PRM approach further revealed that toward higher GOLD stages, the relative contribution of air trapping decreases, whereas the emphysema percentage rises.¹⁹ These key studies emphasize the importance of quantitative postprocessing for imaging-driven research on COPD pathophysiology, not accessible by other noninvasive techniques.

QCT has several limitations that affect quantification of emphysema and also airway geometry. As a limitation related to the imaging technique as such, CT cannot distinguish between mucus and inflammatory airway wall thickening.²³ QCT of the airways is relatively robust against variations in radiation exposure and use of iterative reconstruction, for example, in low-dose CT,²⁹ whereas emphysema values are influenced by radiation exposure.³⁰ Quantitative postprocessing of both the parenchyma and the airways is significantly affected by reconstruction kernels (soft vs. sharp),³¹ reconstructed slice thickness,³² presence of contrast material,^{33–35} and also the type and manufacturer of the CT scanner,³² as well as the actual software algorithm being used.^{12,36} Further, the results depend on the

inspiration level.^{32,37} This effect can be reduced by using spirometrically monitored CT acquisition³⁸ and normalizing the results to the individual lung volume.³⁹ Subsequently, efforts are ongoing to broadly standardize QCT by specific acquisition protocols and reference phantoms, for example, by the SPIROMICS and QIBA initiatives.⁴⁰ In this context, the utility of QCT for COPD phenotyping was demonstrated in the multicenter project EvA (Emphysema vs. Airway disease).³⁹ It was shown that standardization of QCT, achieved by adjusting lung density measurements for lung volume followed by a phantom-based approach, is of critical importance when imaging is acquired from different scanners. The standardization procedure improved the separation of emphysema-dominant from airway-dominant COPD in automated imaging-based phenotyping. However, standardization at present is mainly focused on CT acquisition, and yet does not comprise the software used. Airway walls are small structures compared with the resolution of clinical CT scanners, and, with regard to the different computational algorithms used to segment the airways, simple techniques such as the full width at half maximum method consistently underestimate luminal dimensions and

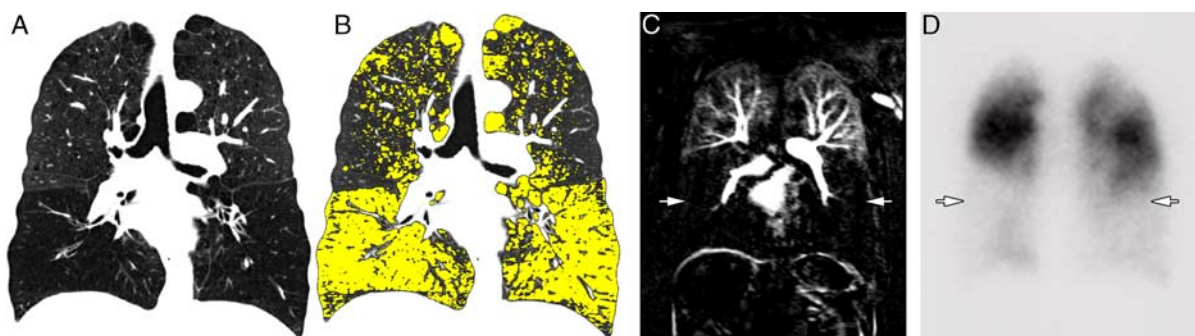


FIGURE 3. CT and MR perfusion scan of a 67-year-old male COPD patient (S7), GOLD status 3. A, CT scan in inspiration. B, Emphysema marked in yellow is mainly localized in the basal lung regions. Insp₋₉₅₀ for the whole lung is 42%, Insp₋₉₅₀ for right upper lobe, right middle lobe, right lower lobe and left upper lobe, left lower lobe is 24%, 60%, 60% and 17%, 58%, respectively. C, 4D Perfusion MRI (TWIST) 15 seconds after contrast injection. D, Coronal projection of lung perfusion scintigraphy. 4D MRI perfusion and perfusion scintigraphy both show matching perfusion defects mainly in the basal lung regions corresponding to the emphysema extent at CT (white arrows). COPD indicates chronic obstructive pulmonary disease.

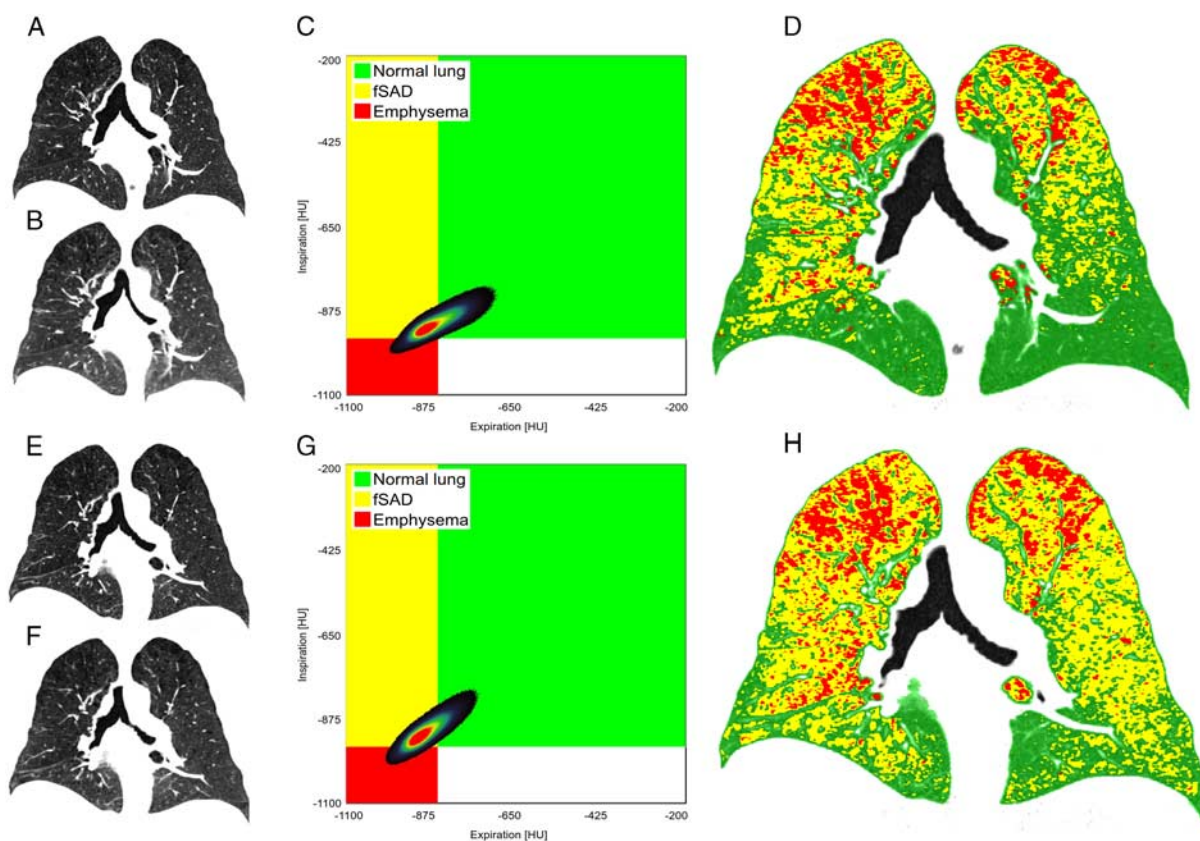


FIGURE 4. CT scan of a 60-year-old male COPD patient (S6). A–D, Baseline scan, GOLD status 2, $FEV_1 = 59\%$. Inspiration scan (A), spatially aligned expiration (B). C, The PRM signature, a frequency distribution, can be calculated by going through every segmented lung voxel and writing the expiration CT value on the x-axis and inspiration CT value on the y-axis. D, $PRM^{Normal} = 58\%$ (green), $PRM^{fSAD} = 33\%$ (yellow), $PRM^{Emph} = 9\%$ (red). E–H, Follow-up scan 3.5 years later, inspiration (E), spatially aligned expiration (F), PRM signature (G), $PRM^{Normal} = 41\%$ (green), $PRM^{fSAD} = 47\%$ (yellow), $PRM^{Emph} = 11\%$ (H) (figure by O. Weinheimer and C.J. Galbán). COPD indicates chronic obstructive pulmonary disease; FEV_1 , forced expiratory volume; PRM, parametric response map.

overestimate wall dimensions, and more sophisticated methods provide more accurate measurements but cannot solve this problem completely.^{24,41}

A relatively new—and even less standardized—approach toward quantifying lung destruction in COPD aims at detecting changes in large and small lung

vasculature. For example, investigators of the MESA study with 2303 participants unselectively quantified the total pulmonary vascular volume and found that a lower vascular volume was associated with a lower cardiac output and dyspnea.⁴² Although the peripheral pulmonary vasculature, determined by the cross-sectional area of vessels $<5\text{ mm}^2$,

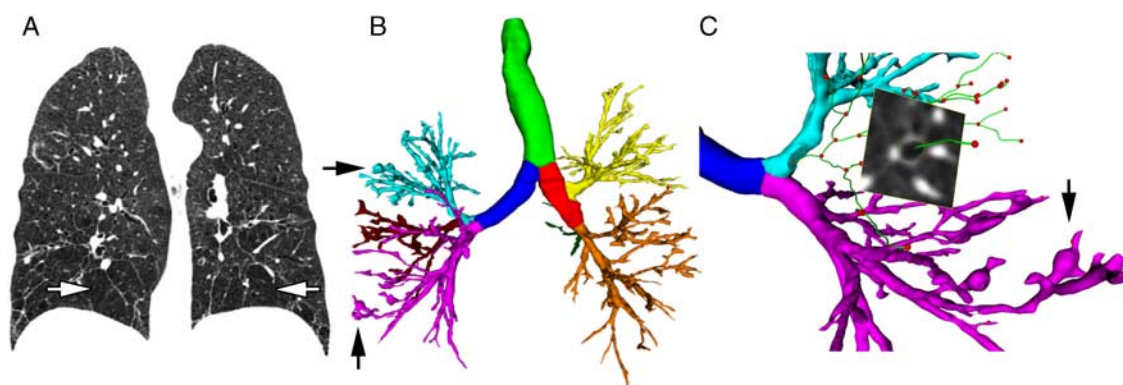


FIGURE 5. A, CT scan of a 61-year-old male COPD patient (S5) with emphysema (white arrows) and bronchiectasis, GOLD status 0. B, Rendering of the labeled tracheobronchial tree, the signs of bronchiectasis are clearly visible (black arrows). C, Example for the determination of lumen and wall area on an orthogonal plane. Taper index calculation helps to quantify the amount of bronchiectasis (black arrow indicates bronchiectasis). COPD indicates chronic obstructive pulmonary disease.

TABLE 1. Recommended Imaging Work-up for Endoscopic Valve Therapy^{17,60,73,74}

Preparation of Endoscopic Valve Therapy	Follow-up After Endoscopic Valve Therapy
CT with slice thickness ≤ 1.25 mm, overlapping reconstructions, obligatory: good inspiratory breath-hold, optional: paired expiratory breath-hold to get a hint for tracheobronchomalacia and a second chance for fissure assessment in case of respiration artifacts Emphysema distribution, quantification, and characterization Software-based postprocessing, lobe-based analysis Exclusion of differential diagnoses pneumonia/tracheobronchomalacia/interstitial lung disease, effusion, severe bronchiectasis, compressive atelectasis, and pulmonary embolism Exclusion of nodules and severe pleural adhesions of target lobe Detailed fissure analysis, endoscopic measurement of collateral ventilation might be used additionally Lung perfusion study (scintigraphy or SPECT) or perfusion CT or MRI Selection of target lobe with high emphysema index $>40\%$ and matching perfusion deficit	Same-day chest x-ray in 2 planes Depending on the clinical course, regular x-ray to control valve position, evaluate volume reduction, and check for complications (eg, pneumothorax) If absence of clinical improvement and/or lobar atelectasis on chest x-ray, thin-section CT to control for volume reduction, verification of optimal valve localization in relation to subsegmental bronchi, which might be out of sight in bronchoscopy, optimal fitting inside the occluded bronchi, and minimal valve displacement

may hypothetically decrease in parallel to increasing emphysematous destruction in COPD, the interaction may be more complex and may also depend on hypoxic pulmonary vasoconstriction.^{43,44} As main pulmonary arterial enlargement, in contrast, is associated with COPD exacerbation and mortality,⁴⁵ it will be critical to study the changes on the different levels of vasculature just as it is required in airway quantification.

ENDOBONCHIAL THERAPIES

Traditionally, in subjects with upper lobe–predominant emphysema, lung volume reduction surgery (LVRS) can improve exercise performance and quality of life and presents a survival-enhancing therapy.⁴⁶ Thereby, the most diseased portions of the lungs are resected, leading to hyperinflation reduction, and thus optimizing respiratory mechanics. Besides conventional LVRS, bullectomy is still the treatment of choice of giant bullae. Size and location of bullae should be reported by the radiologist as well as substantial compression of adjacent lung tissue.⁴⁶ In cases wherein the bulla occupies at least one-third of the hemithorax with subsequent compression of adjacent lung tissue, bullectomy was shown to substantially improve dyspnea and lung function.⁴⁶

In the last 15 years, various endoscopic techniques were developed, extending the therapeutic spectrum for patients with advanced COPD and emphysema. The physiological effect of the various ELVR techniques is comparable to that of LVRS but with a potentially better risk profile. The success of the different endoscopic treatment modalities depends on precise patient selection. Moreover, an estimated half of the emphysema patients will not benefit from any interventional techniques and should be excluded from these therapeutic modalities. The decision for an invasive treatment approach and the type of intervention (endobronchial therapy, LVRS) should be discussed for each individual emphysema patient within the context of a multidisciplinary team including pneumologists, radiologists, and thoracic surgeons.

The severity of airflow limitation, hyperinflation, emphysema distribution, and interlobar fissure integrity present the key factors that contribute to the decision for an invasive treatment approach. The most important examinations to identify candidates for endobronchial emphysema therapies or LVRS include body plethysmography and high-resolution CT.⁴⁷ Symptomatic emphysema patients despite

maximal pharmacological therapy with a FEV1 between 20% and 45% predicted and a residual volume $>175\%$ predicted may be considered as candidates for any interventional therapy. Moreover, noncontrast volumetric CT scan with a slice thickness of 0.5 to 1.25 mm and overlapping reconstructions is required to characterize the emphysema severity, emphysema distribution, and interlobar fissure integrity that is a surrogate for interlobar collateral ventilation (CV), as described below (Table 1).

In general, the endoscopic interventions that aim at hyperinflation reduction are divided into blocking and nonblocking ELVR techniques that aim at hyperinflation reduction. The blocking technique is represented by the reversible valve therapy, whereas the nonblocking technique includes the coil therapy, the polymeric lung volume reduction (PLVR), and bronchoscopic thermal vapor ablation (BTVA). One of the most important differences between the blocking and the nonblocking devices is their dependence on interlobar CV. Although only patients with a complete fissure and thus absent CV will benefit from valve therapy, patients with an incomplete fissure and thus significant CV do not benefit from valve treatment, as the occluded lobe can be backfilled through the collateral channels. In this context, incomplete interlobar fissures are frequently observed on CT scans among the general population with 17% to 85% for the right major fissure, 19% to 74% for the left major fissure, and 20% to 90% for the minor fissure and allow for substantial air flow to a neighboring lobe.⁴⁸ Nowadays, a complete fissure that indicates no or negligible interlobar CV is defined as $>95\%$ completeness of the fissure between the target and adjacent lobes on at least one axis of the CT scan.⁴⁸ Besides CT fissure analysis, CV can be quantified endoscopically by using the Chartis Pulmonary Assessment system. Thereby, a catheter with an inflatable balloon at the distal tip is inserted into the targeted lobe. After isolating the most diseased lung lobe by inflating the balloon, the airflow can be measured, and thus CV can be quantified. Besides their distinction in CV dependence, the valve therapy differs from the nonblocking ELVR methods by its reversibility.

Valve Therapy

By complete occlusion of the most emphysematous lung lobe by 1-way valves, a lobar atelectasis occurs, and it results in the desired partial lung volume reduction in selected emphysema patients with absent interlobar CV

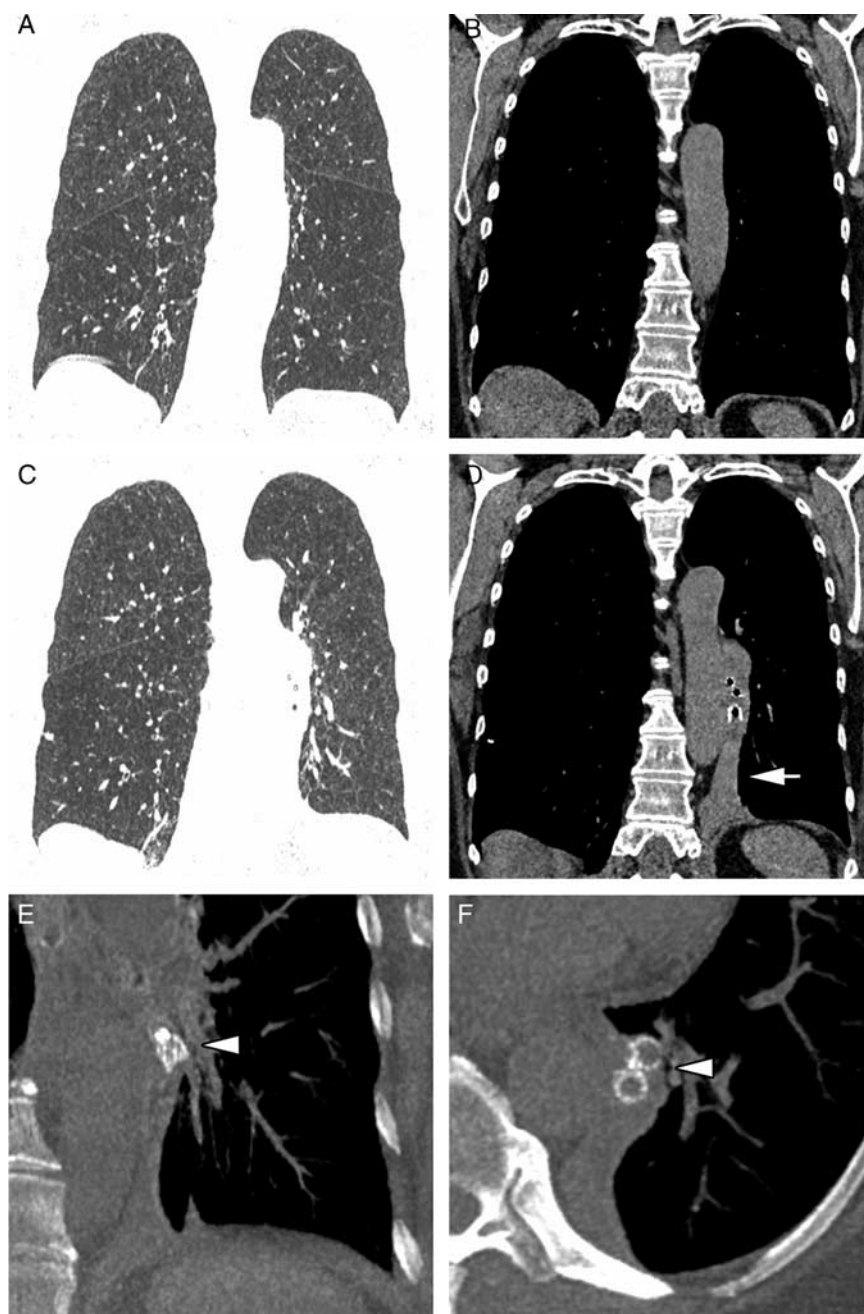


FIGURE 6. A and B, Endobronchial valve therapy in a 64-year-old woman. CT showed lower lobe–predominant emphysema. Major fissures were > 95% complete in a visual assessment. C and D, Repeat CT 3 months following implantation of endobronchial valves in the left lower lobe (white arrowheads), which resulted in complete lower lobe atelectasis (white arrow). E and F, Magnified maximum intensity projections of the valves implanted into the segmental bronchi of the left lower lobe (white arrowheads indicates valves).

(Fig. 6). Two different types of valves in different sizes are available that are distinguished by shape, but both act as 1-way valves. The type of valve and the size of the valve are selected depending on the anatomy and diameter of the bronchi of the target lobe. So far, the efficacy of valve therapy was evaluated in several published randomized controlled trials (RCT).^{49–57} In the first RCTs, statistically significant improvement of lung function parameters, exercise capacity, and health-related quality of life was observed but was of uncertain clinical importance. In these trials,

however, patients were enrolled irrespective of the interlobar CV and/or treated by incomplete occlusion of the lung lobe.^{49–52} Post hoc analysis, however, identified a complete occlusion of the target lobe and an absent CV as important prerequisites for a clinically relevant benefit following valve placement. Therefore, only patients with absent CV that was confirmed by CT fissure analysis or invasive CV measurement by the Chartis System were enrolled in the recent RCTs that showed the valve therapy to result in clinically relevant benefit.^{53–57} Moreover, retrospective trials showed

that valve therapy is associated with a survival benefit in patients who experienced a lobar atelectasis following valve implantation.^{58,59} Although valve therapy is a minimally invasive treatment, it can be accompanied by adverse events. The most common complication with a rate of 18% to 29% is a pneumothorax due to lobar volume shift after valve placement that requires a chest tube insertion in the majority of the patients with pneumothorax (Table 1). Valve removal or, in rare cases, surgical intervention may also be necessary for pneumothorax management. Nevertheless, pneumothorax does not seem to impact the clinical status in the majority of patients and is even associated with superior outcome in patients in whom complete lobar atelectasis can be observed after their recovery from pneumothorax.⁶⁰

Nonblocking ELVR Techniques

Besides the blocking valve therapy, the nonblocking techniques consisting of coil therapy, BTVA, and PLVR aim at hyperinflation reduction in patients with advanced emphysema. The most significant difference to the valve therapy is their independence of CV, but also their irreversibility. The major concern with the nonblocking techniques is the insufficient knowledge about predictors of a successful outcome. The coil therapy consists of implantation of a number of lung volume reduction coils in the target lobe, leading to parenchymal compression, and thus to lobe volume reduction and improvement of lung elastic recoil (Fig. 7). So far, 3 RCTs confirmed the efficacy of coil therapy in improving lung function parameters, exercise capacity, and quality of life.^{61–63} Although achieving statistical significance, the clinical benefit was nevertheless only modest and of uncertain clinical importance. Therefore, coil therapy should preferably be performed within clinical trials. The BTVA and PLVR are similar endobronchial approaches, as both induce an inflammatory reaction that leads to fibrosis and shrinkage and thus to lung volume reduction. BTVA is a segmental treatment approach in patients with upper lobe predominant emphysema, whereby heated water vapor is installed in the most emphysematous segments. The PLVR uses a synthetic polymer in the emphysematous lung areas to promote inflammation and lung volume reduction. The efficacy of both methods is confirmed in one RCT that indicates encouraging improvements in major COPD outcome parameters.^{64,65} The most common adverse events following BTVA and PLVR are COPD exacerbations, pneumonitis, and pneumonia. Particularly, PLVR is associated with a high-risk profile that limits its current utility. As the data for BTVA and PLVR are still very limited, these methods should be used within clinical trials.

Targeted Lung Denervation (TLD)

Besides ELVR, the TLD presents an endoscopic treatment approach that aims at sustainable bronchodilation by ablation of parasympathetic pulmonary nerves. As TLD does not aim at hyperinflation reduction, it may present a treatment modality in patients with airway and emphysema-dominant phenotypes. During an endoscopic procedure, a dedicated catheter is advanced into the main bronchi. Afterward, radiofrequency energy is delivered to ablate the pulmonary nerves. Thereby, TLD is performed bilaterally in both main bronchi in a single procedure. The first trial related to TLD confirmed the safety and feasibility of this technique and demonstrated encouraging efficacy results.⁶⁶ So far, TLD is still under investigation, and the results of an RCT are still pending.

STRATIFICATION FOR NOVEL THERAPIES

Novel therapies increase the spectrum of therapeutic options in COPD, but they also require sophisticated diagnostics in terms of preprocedural phenotyping and postprocedural monitoring. In addition to clinical tests providing global information on airflow limitation, CT-based information on the extent of regional hyperinflation, emphysema, airway geometry/stability, and fissure integrity becomes increasingly important for the selection of appropriate treatment for individuals, thus increasing treatment success and avoiding unnecessary therapies.

With regard to implantation of endobronchial 1-way valves, regional emphysema severity should be reported for individual lung lobes instead of nonanatomic lung regions, as a unilateral upper or lower lobar target with sufficient severity warranting total atelectasis has to be identified, whereas the presence of sufficient emphysema heterogeneity supports the preservation of a less severely affected adjacent ipsilateral lobe (Fig. 6).⁴⁹ Visual rating scales allow for semistandardized reporting of local emphysema extent in percentage of the lobar and total lung volume.^{16,67} Quantitative software, however, allows for a more objective assessment, and several software tools have already succeeded in automatic lobar segmentations with subsequent lobar analysis of emphysema and air-trapping extent, even in subjects with incomplete fissures with relatively low bias,^{12–14} thus improving accuracy in patient selection for clinical studies or selection of treatment (Fig. 7).

A visual assessment of fissure integrity can be easily performed using low-dose noncontrast chest CT scans with thin-section reconstructions. However, due to the disturbance of lung architecture with substantial distortion of fissures, visual assessments solely based on axial images may incorrectly characterize fissural defects. Therefore, additional sagittal and coronal image reconstructions are mandatory. In this context, studies have shown variable (ie, fair to moderate, $\kappa=0.59$ to 0.76) interobserver agreement among experienced radiologists concerning the detection of incomplete fissures.^{16,68} The percentage of incompleteness should be also reported for each fissure. The automatic software was also shown to detect and quantify structural defects of fissures, with similar accuracy as expert radiologists.⁶⁹ Although CT analyses of fissure integrity represent indirect measurements (ie, surrogate parameters), the extent of CV can be measured directly with endobronchial balloon catheter systems such as Chartis (PulmonX Inc., Redwood City, CA). However, these systems have certain limitations depending on bronchial anatomy. For example, it is challenging to include the B6 bronchus of the left lower lobe in the measurements.⁷⁰ On comparing Chartis and CT with surgical inspections serving as the standard of reference, both modalities showed a moderate accuracy (71% vs. 76%) for the detection of incomplete fissures.⁷¹ Defining completeness as 90% of the fissure being visible and treatment success as lung volume reduction of at least 350 mL, CT and Chartis showed similar accuracy (77% vs. 74%) in the prediction of response to valve treatment.⁷² Importantly, the response to valve treatment can be predicted more accurately when combining CT and Chartis.⁴⁸ Valve therapy monitoring is initially performed using high-quality chest x-ray, which can sufficiently show the localization of the valves and the advent of lobar atelectasis, but also complications such as pneumothorax. If clinical benefit does not occur, further imaging with CT is required in order to quantify target lobe volume reduction and to detect valve migration and malpositioning in more detail at 3 or

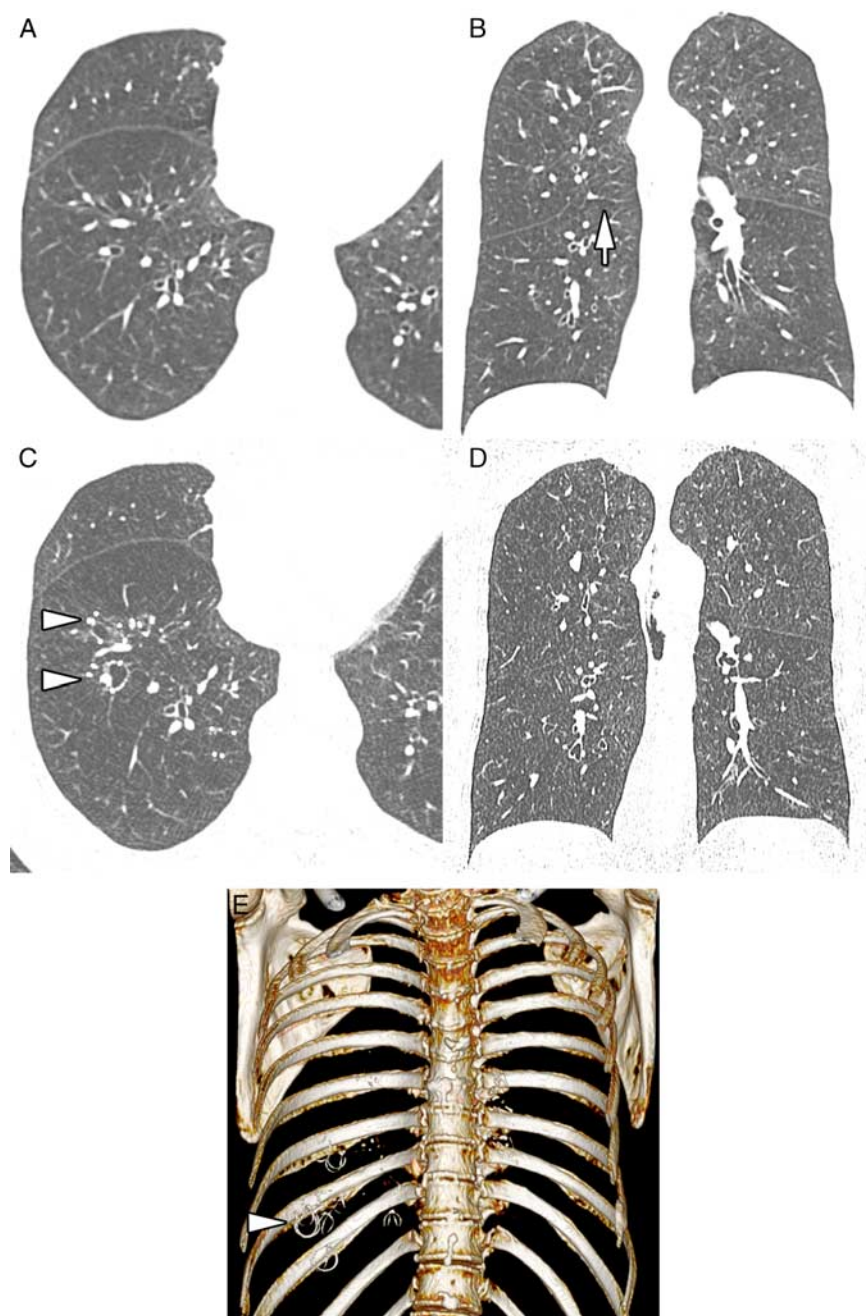


FIGURE 7. Endobronchial coil therapy in a 60-year-old woman. A and B, Preprocedural work-up revealed severe centrilobular emphysema with highest severity in the right lower lobe, which, however, showed a large gap in the oblique fissure with the upper lobe (white arrow) (B). C–E, Subsequently, endoscopic lung volume reduction using coil implantation (white arrowheads) was performed. These led to elastic deformation of the subsegmental airways with adjacent parenchyma (C).

6 months following valve placement (Table 1).^{17,60,73,74} Furthermore, a CT scan with contrast medium is recommended if emphysema patients with a valve-induced lobar atelectasis present clinical signs of infection to confirm/exclude post-obstructive pneumonia.

Today, an increasing number of pharmaceutical studies on innovative anti-inflammatory or enzyme-inhibiting agents is being performed using quantitative CT or innovative MRI techniques as part of study protocols. In this context, imaging is used not only for patient selection but also for patient

monitoring. For example, airway response to anti-inflammatory therapy with Roflumilast has been investigated in a randomized controlled study (ClinicalTrials.gov identifier: NCT01480661) in patients with severe COPD, with quantitative CT of the airways (including air-flow simulations) serving as the primary outcome measure, providing information on airway geometry and function. In a prospective, randomized, placebo-controlled study (ClinicalTrials.gov identifier: NCT02722304), the safety and efficacy of alpha1-proteinase Inhibitor (A1PI) augmentation therapy in subjects with A1PI

deficiency and COPD is currently investigated, and the primary outcome measures of the study include longitudinal changes in CT lung density. However, therapy monitoring in COPD based on CT measures of emphysema is challenging, as the measured annual emphysema progression rate is relatively low. For example, in the Multi-Ethnic Study of Atherosclerosis (MESA) lung study including >4000 subjects with a high percentage of smokers, the median percent emphysema (threshold, −950 HU) was 3.0% at baseline, and the rate of progression was 0.64 percentage points over a median of 9.3 years.⁷⁵ A mean annual increase of emphysema (−950 HU) of 1.07% was found by Mohamed Hoesin et al⁷⁶ in a cohort of 3670 former and current smokers. Smaller studies among COPD patients reported annual progression rates in percent emphysema of up to 1.03 percentage points depending on the smoking status.^{77–79} Moreover, the magnitude of the reported long-term changes is within the limits of reported short-term variability.⁸⁰ Interestingly, the smoking status was shown to significantly influence quantitative CT measures of both lung tissue density and potentially airway geometry.^{79,81} Therefore, such effects of smoking cessation should be considered when using quantitative CT for therapy monitoring. Longitudinal data on quantitative assessments of airway geometry or air trapping are still lacking. However, preliminary data could show therapy response to bronchodilators, indicating that CT-derived imaging biomarkers of airway remodeling for clinical studies addressing the airway-dominant phenotype of COPD might be more effective as endpoints compared with using low-attenuation areas in emphysema-dominant COPD.⁸²

Tracheal collapse in both patients with stable COPD and patients with disease exacerbation is considerably more prevalent than in healthy individuals.⁸³ In this particular phenotype of COPD, common symptoms include dyspnea, constant coughing, inability to raise secretions, and recurrent respiratory infections.⁸⁴ Hence, it should be part of comprehensive COPD evaluation and management.⁸³ In addition to dynamic CT, awake functional bronchoscopy and pulmonary function studies are recommended in these patients.⁸⁴ In this context, it was shown that the magnitude of static end-expiratory tracheal collapse (on expiratory CT) does not predict excessive dynamic expiratory tracheal collapse, as it can occur at variable timepoints during the respiratory cycle.⁸⁵ This can be addressed with cine CT, which nicely depicts dynamic airway collapse but is limited to predefined anatomical positions.⁸⁶ Low-dose dynamic respiratory-gated multidetector CT (4D-CT) of the whole chest is now readily available to simultaneously assess the dynamic collapse of any part of the tracheobronchial tree, as well as respiratory dynamics.⁸⁶ It is acquired during regular tidal breathing and provides thin-section reconstruction, low z-axis increment, and low (5%) respiratory increment at low radiation exposure comparable to paired low-dose CT examinations.⁸⁶ In patients with significant associated symptoms and severe collapse on CT, temporary Y-shaped airway stent implantation can be considered. However, as airway stents are often associated with complications such as secretion retention, stent implantation does not present a definitive treatment in patients with severe airway instability. In case of symptom relief after stent implantation, the stent should be removed, and patients are considered for surgical reconstruction (membranous wall plication) through a right thoracotomy to improve patient symptoms and quality of life.⁸⁴ Besides, information from 4D-CT may also be useful for the planning of lung volume reduction therapies.

As a critical note, CT-based biomarkers of lung structure and function enjoy increasing popularity, but substantial intercenter variability can be found due to heterogeneity of imaging protocols or imaging equipment, as discussed above.³² Although reported differences resulting from aforementioned factors along the chain of generating quantitative information from image data are rather subtle, they often are within the same order of magnitude as reported longitudinal changes for emphysema or clinically meaningful variations in airway wall metrics.

CONCLUSIONS

The differentiation of emphysema-dominant and airway-dominant COPD phenotypes has immediate practical value in routine patient care with regard to therapy selection. A precise morphologic characterization of emphysema severity, distribution patterns, and fissure completeness supported by software-generated quantitative indices are key to assign patients with advanced emphysema to modern mainly endoscopic techniques for lung volume reduction. With regard to earlier stage COPD, it is less clear to which extent quantitative CT plays a role for therapy selection and as an outcome measure, as natural emphysema progression is slow, which makes it a problematic target for drug trials, and longitudinal data on quantitative airway metrics is currently missing, which requires further research in order to set up new endpoints.

REFERENCES

1. Vogelmeier CF, Criner GJ, Martinez FJ, et al. Global strategy for the diagnosis, management, and prevention of chronic obstructive lung disease 2017 report. GOLD executive summary. *Am J Respir Crit Care Med*. 2017;195:557–582.
2. Jorres RA, Welte T, Bals R, et al. Systemic manifestations and comorbidities in patients with chronic obstructive pulmonary disease (COPD) and their effect on clinical state and course of the disease—an overview of the cohort study COSYCONET. *Dtsch Med Wochenschr*. 2010;135:446–449.
3. Regan EA, Hokanson JE, Murphy JR, et al. Genetic epidemiology of COPD (COPDGene) study design. *COPD*. 2011;7:32–43.
4. Lynch DA, Austin JHM, Hogg JC, et al. CT-definable subtypes of chronic obstructive pulmonary disease: a statement of the Fleischner Society. *Radiology*. 2015;277:192–205.
5. Kauczor HU, Wielpütz MO, Owsijewitsch M, et al. Computed tomographic imaging of the airways in COPD and asthma. *J Thorac Imaging*. 2011;26:290–300.
6. Gevenois PA, De Vuyst P, de Maertelaer V, et al. Comparison of computed density and microscopic morphometry in pulmonary emphysema. *Am J Respir Crit Care Med*. 1996;154:187–192.
7. Coxson HO, Mayo J, Lam S, et al. New and current clinical imaging techniques to study chronic obstructive pulmonary disease. *Am J Respir Crit Care Med*. 2009;180:588–597.
8. Stern EJ, Müller NL, Swensen SJ, et al. CT mosaic pattern of lung attenuation: etiologies and terminology. *J Thorac Imaging*. 1995;10:294–297.
9. Hansell DM, Bankier AA, MacMahon H, et al. Fleischner Society: glossary of terms for thoracic imaging. *Radiology*. 2008;246:697–722.
10. Newell JD Jr, Sieren J, Hoffman EA. Development of quantitative computed tomography lung protocols. *J Thorac Imaging*. 2013;28:266–271.
11. Hersh CP, Washko GR, Estepar RS, et al. Paired inspiratory-expiratory chest CT scans to assess for small airways disease in COPD. *Respir Res*. 2013;14:42.

12. Lim HJ, Weinheimer O, Wielpütz MO, et al. Fully automated pulmonary lobar segmentation: influence of different prototype software programs onto quantitative evaluation of chronic obstructive lung disease. *PLoS One*. 2016;11:e0151498.
13. Müller J, Lim HJ, Eichinger M, et al. Influence of fissure integrity on quantitative CT and emphysema distribution in emphysema-type COPD using a dedicated COPD software. *Eur J Radiol*. 2017;95:293–299.
14. Konietzke P, Weinheimer O, Wielpütz MO, et al. Validation of automated lobe segmentation on paired inspiratory-expiratory chest CT in 8-14 year-old children with cystic fibrosis. *PLoS One*. 2018;13:e0194557.
15. Criner GJ, Sternberg AL. A clinician's guide to the use of lung volume reduction surgery. *Proc Am Thorac Soc*. 2008;5:461–467.
16. Koenigkam-Santos M, de Paula WD, Owsijewitsch M, et al. Incomplete pulmonary fissures evaluated by volumetric thin-section CT: semi-quantitative evaluation for small fissure gaps identification, description of prevalence and severity of fissural defects. *Eur J Radiol*. 2013;82:2365–2370.
17. Gompelmann D, Sarmand N, Herth FJ. Interventional pulmonology in chronic obstructive pulmonary disease. *Curr Opin Pulm Med*. 2017;23:261–268.
18. Matsuoka S, Kurihara Y, Yagihashi K, et al. Quantitative assessment of air trapping in chronic obstructive pulmonary disease using inspiratory and expiratory volumetric MDCT. *AJR Am J Roentgenol*. 2008;190:762–769.
19. Galbán CJ, Han MK, Boes JL, et al. Computed tomography-based biomarker provides unique signature for diagnosis of COPD phenotypes and disease progression. *Nat Med*. 2012;18:1711–1715.
20. Regan EA, Hokanson JE, Murphy JR, et al. Genetic epidemiology of COPD (COPDGene) study design. *COPD*. 2010;7:32–43.
21. Couper D, LaVange LM, Han M, et al. Design of the subpopulations and intermediate outcomes in COPD study (SPIROMICS). *Thorax*. 2014;69:491–494.
22. Goris ML, Zhu HJ, Blankenberg F, et al. An automated approach to quantitative air trapping measurements in mild cystic fibrosis. *Chest*. 2003;123:1655–1663.
23. Achenbach T, Weinheimer O, Biedermann A, et al. MDCT assessment of airway wall thickness in COPD patients using a new method: correlations with pulmonary function tests. *Eur Radiol*. 2008;18:2731–2738.
24. Weinheimer O, Achenbach T, Bletz C, et al. About objective 3-d analysis of airway geometry in computerized tomography. *IEEE Trans Med Imaging*. 2008;27:64–74.
25. Weinheimer O, Wielpütz MO, Konietzke P, et al. Fully automated lobe-based airway taper index calculation in a low dose MDCT CF study over 4 time-points. *SPIE Med Imaging*. 2017;U101330–U101339.
26. Grydeland TB, Dirksen A, Coxson HO, et al. Quantitative computed tomography: emphysema and airway wall thickness by sex, age and smoking. *Eur Respir J*. 2009;34:858–865.
27. Martinez CH, Chen YH, Westgate PM, et al. Relationship between quantitative CT metrics and health status and BODE in chronic obstructive pulmonary disease. *Thorax*. 2012;67:399–406.
28. Han MK, Kazerooni EA, Lynch DA, et al. Chronic obstructive pulmonary disease exacerbations in the COPDGene study: associated radiologic phenotypes. *Radiology*. 2011;261:274–282.
29. Leutz-Schmidt P, Weinheimer O, Jobst BJ, et al. Influence of exposure parameters and iterative reconstruction on automatic airway segmentation and analysis on MDCT—An ex vivo phantom study. *PLoS One*. 2017;12:e0182268.
30. Zaporozhan J, Ley S, Weinheimer O, et al. Multi-detector CT of the chest: influence of dose onto quantitative evaluation of severe emphysema: a simulation study. *J Comput Assist Tomogr*. 2006;30:460–468.
31. Ley-Zaporozhan J, Ley S, Weinheimer O, et al. Quantitative analysis of emphysema in 3D using MDCT: influence of different reconstruction algorithms. *Eur J Radiol*. 2008;65:228–234.
32. Zach JA, Newell JD Jr, Schroeder J, et al. Quantitative computed tomography of the lungs and airways in healthy nonsmoking adults. *Invest Radiol*. 2012;47:596–602.
33. Heussel CP, Kappes J, Hantusch R, et al. Contrast enhanced CT-scans are not comparable to non-enhanced scans in emphysema quantification. *Eur J Radiol*. 2009;74:473–478.
34. Wielpütz MO, Hintze C, Jobst B, et al. Influence of contrast media on computational airway analysis on MDCT. *J Thorac Imaging*. 2012;27:W128.
35. Dettmer S, Entrup J, Schmidt M, et al. Bronchial wall thickness measurement in computed tomography: effect of intravenous contrast agent and reconstruction kernel. *Eur J Radiol*. 2012;81:3606–3613.
36. Wielpütz MO, Bardarova D, Weinheimer O, et al. Variation of densitometry on computed tomography in COPD—influence of different software tools. *PLoS One*. 2014;9:e112898.
37. Ley-Zaporozhan J, Ley S, Mews J, et al. Changes of emphysema parameters over the respiratory cycle during free breathing: preliminary results using respiratory gated 4D-CT. *COPD*. 2017;14:597–602.
38. Salamon E, Lever S, Kuo W, et al. Spirometer guided chest imaging in children: it is worth the effort! *Pediatr Pulmonol*. 2017;52:48–56.
39. Subramanian DR, Gupta S, Burggraf D, et al. Emphysema- and airway-dominant COPD phenotypes defined by standardised quantitative computed tomography. *Eur Respir J*. 2016;48:92–103.
40. Sieren JP, Newell JD Jr, Barr RG, et al. SPIROMICS protocol for multicenter quantitative computed tomography to phenotype the lungs. *Am J Respir Crit Care Med*. 2016;194:794–806.
41. Hackx M, Bankier AA, Gevenois PA. Chronic obstructive pulmonary disease: CT quantification of airways disease. *Radiology*. 2012;265:34–48.
42. Aaron CP, Hoffman EA, Lima JAC, et al. Pulmonary vascular volume, impaired left ventricular filling and dyspnea: the MESA lung study. *PLoS One*. 2017;12:e0176180.
43. Takayanagi S, Kawata N, Tada Y, et al. Longitudinal changes in structural abnormalities using MDCT in COPD: do the CT measurements of airway wall thickness and small pulmonary vessels change in parallel with emphysematous progression? *Int J Chron Obstruct Pulmon Dis*. 2017;12:551–560.
44. Mashimo S, Chubachi S, Tsutsumi A, et al. Relationship between diminution of small pulmonary vessels and emphysema in chronic obstructive pulmonary disease. *Clin Imaging*. 2017;46:85–90.
45. Wells JM, Washko GR, Han MK, et al. Pulmonary arterial enlargement and acute exacerbations of COPD. *N Engl J Med*. 2012;367:913–921.
46. Marchetti N, Criner GJ. Surgical approaches to treating emphysema: lung volume reduction surgery, bullectomy, and lung transplantation. *Semin Respir Crit Care Med*. 2015;36:592–608.
47. Herth FJF, Slebos DJ, Criner GJ, et al. Endoscopic lung volume reduction: an expert panel recommendation—update 2017. *Respiration*. 2017;94:380–388.
48. Koster TD, van Rikxoort EM, Huebner RH, et al. Predicting lung volume reduction after endobronchial valve therapy is maximized using a combination of diagnostic tools. *Respiration*. 2016;92:150–157.
49. Sciruba FC, Ernst A, Herth FJ, et al. A randomized study of endobronchial valves for advanced emphysema. *N Engl J Med*. 2010;363:1233–1244.
50. Herth FJ, Noppen M, Valipour A, et al. Efficacy predictors of lung volume reduction with Zephyr valves in a European cohort. *Eur Respir J*. 2012;39:1334–1342.
51. Ninane V, Geltner C, Bezzi M, et al. Multicentre European study for the treatment of advanced emphysema with bronchial valves. *Eur Respir J*. 2012;39:1319–1325.
52. Wood DE, Nader DA, Springmeyer SC, et al. The IBV Valve trial: a multicenter, randomized, double-blind trial of endobronchial therapy for severe emphysema. *J Bronchol Interv Pulmonol*. 2014;21:288–297.

53. Davey C, Zoumot Z, Jordan S, et al. Bronchoscopic lung volume reduction with endobronchial valves for patients with heterogeneous emphysema and intact interlobar fissures (the BeLieveR-HiFi study): a randomised controlled trial. *Lancet*. 2015;386:1066–1073.
54. Klooster K, ten Hacken NH, Hartman JE, et al. Endobronchial valves for emphysema without interlobar collateral ventilation. *N Engl J Med*. 2015;373:2325–2335.
55. Valipour A, Slebos DJ, Herth F, et al. Endobronchial valve therapy in patients with homogeneous emphysema. Results from the IMPACT Study. *Am J Respir Crit Care Med*. 2016;194:1073–1082.
56. Kemp SV, Slebos DJ, Kirk A, et al. A multicenter randomized controlled trial of Zephyr endobronchial valve treatment in heterogeneous emphysema (TRANSFORM). *Am J Respir Crit Care Med*. 2017;196:1535–1543.
57. Criner GJ, Sue R, Wright S, et al. A multicenter RCT of Zephyr(R) endobronchial valve treatment in heterogeneous emphysema (LIBERATE). *Am J Respir Crit Care Med*. 2018;198:1151–1164.
58. Hopkinson NS, Kemp SV, Toma TP, et al. Atelectasis and survival after bronchoscopic lung volume reduction for COPD. *Eur Respir J*. 2011;37:1346–1351.
59. Venuta F, Anile M, Diso D, et al. Long-term follow-up after bronchoscopic lung volume reduction in patients with emphysema. *Eur Respir J*. 2012;39:1084–1089.
60. Gompelmann D, Benjamin N, Kontogianni K, et al. Clinical and radiological outcome following pneumothorax after endoscopic lung volume reduction with valves. *Int J Chron Obstruct Pulmon Dis*. 2016;11:3093–3099.
61. Shah PL, Zoumot Z, Singh S, et al. Endobronchial coils for the treatment of severe emphysema with hyperinflation (RESET): a randomised controlled trial. *Lancet Respir Med*. 2013;1:233–240.
62. Deslee G, Klooster K, Hetzel M, et al. Lung volume reduction coil treatment for patients with severe emphysema: a European multicentre trial. *Thorax*. 2014;69:980–986.
63. Scirba FC, Criner GJ, Strange C, et al. Effect of endobronchial coils vs usual care on exercise tolerance in patients with severe emphysema: the RENEW Randomized Clinical Trial. *JAMA*. 2016;315:2178–2189.
64. Herth FJ, Valipour A, Shah PL, et al. Segmental volume reduction using thermal vapour ablation in patients with severe emphysema: 6-month results of the multicentre, parallel-group, open-label, randomised controlled STEP-UP trial. *Lancet Respir Med*. 2016;4:185–193.
65. Come CE, Kramer MR, Dransfield MT, et al. A randomised trial of lung sealant versus medical therapy for advanced emphysema. *Eur Respir J*. 2015;46:651–662.
66. Slebos DJ, Klooster K, Koegelenberg CF, et al. Targeted lung denervation for moderate to severe COPD: a pilot study. *Thorax*. 2015;70:411–419.
67. Fahndrich S, Biertz F, Karch A, et al. Cardiovascular risk in patients with alpha-1-antitrypsin deficiency. *Respir Res*. 2017;18:171.
68. Guan CS, Xu Y, Han D, et al. Volumetric thin-section CT: evaluation of pulmonary interlobar fissures. *Diagn Interv Radiol*. 2015;21:466–470.
69. van Rikxoort EM, Goldin JG, Galperin-Aizenberg M, et al. A method for the automatic quantification of the completeness of pulmonary fissures: evaluation in a database of subjects with severe emphysema. *Eur Radiol*. 2012;22:302–309.
70. Koster TD, Slebos DJ. The fissure: interlobar collateral ventilation and implications for endoscopic therapy in emphysema. *Int J Chronic Obstruct Pulmon Dis*. 2016;11:765–773.
71. Diso D, Anile M, Carillo C, et al. Correlation between collateral ventilation and interlobar lung fissures. *Respiration*. 2014;88:315–319.
72. Gompelmann D, Eberhardt R, Slebos DJ, et al. Diagnostic performance comparison of the Chartis System and high-resolution computerized tomography fissure analysis for planning endoscopic lung volume reduction. *Respirology*. 2014;19:524–530.
73. Gompelmann D, Kontogianni K, Schuhmann M, et al. The minimal important difference for target lobe volume reduction after endoscopic valve therapy. *Int J Chron Obstruct Pulmon Dis*. 2018;13:465–472.
74. Gompelmann D, Gerovasili V, Kontogianni K, et al. Endoscopic valve removal >180 days since implantation in patients with severe emphysema. *Respiration*. 2018;96:348–354.
75. Parikh MA, Aaron CP, Hoffman EA, et al. Angiotensin-converting inhibitors and angiotensin ii receptor blockers and longitudinal change in percent emphysema on computed tomography. The Multi-Ethnic Study of Atherosclerosis Lung Study. *Ann Am Thorac Soc*. 2017;14:649–658.
76. Mohamed Hoessein FA, Zanen P, de Jong PA, et al. Rate of progression of CT-quantified emphysema in male current and ex-smokers: a follow-up study. *Respir Res*. 2013;14:55.
77. Tanabe N, Muro S, Sato S, et al. Longitudinal study of spatially heterogeneous emphysema progression in current smokers with chronic obstructive pulmonary disease. *PloS One*. 2012;7:e44993.
78. Bhavani S, Tsai CL, Perusich S, et al. Clinical and immunological factors in emphysema progression. Five-year prospective longitudinal exacerbation study of chronic obstructive pulmonary disease (LES-COPD). *Am J Respir Crit Care Med*. 2015;192:1171–1178.
79. Jobst BJ, Weinheimer O, Trauth M, et al. Effect of smoking cessation on quantitative computed tomography in smokers at risk in a lung cancer screening population. *Eur Radiol*. 2018;28:807–815.
80. Kauczor HU, Heussel CP, Herth FJ. Longitudinal quantitative low-dose CT in COPD: ready for use? *Lancet Respir Med*. 2013;1:95–96.
81. Zach JA, Williams A, Jou SS, et al. Current smoking status is associated with lower quantitative CT measures of emphysema and gas trapping. *J Thorac Imaging*. 2016;31:29–36.
82. Hasegawa M, Makita H, Nasuhara Y, et al. Relationship between improved airflow limitation and changes in airway calibre induced by inhaled anticholinergic agents in COPD. *Thorax*. 2009;64:332–338.
83. Leong P, Tran A, Rangaswamy J, et al. Expiratory central airway collapse in stable COPD and during exacerbations. *Respir Res*. 2017;18:163.
84. Wright CD. Tracheobronchomalacia and expiratory collapse of central airways. *Thorac Surg Clin*. 2018;28:163–166.
85. O'Donnell CR, Bankier AA, O'Donnell DH, et al. Static end-expiratory and dynamic forced expiratory tracheal collapse in COPD. *Clin Radiol*. 2014;69:357–362.
86. Wielpütz MO, Eberhardt R, Puderbach M, et al. Simultaneous assessment of airway instability and respiratory dynamics with low-dose 4D-CT in chronic obstructive pulmonary disease: a technical note. *Respiration*. 2014;87:294–300.